Available online at www.sciencedirect.com

ScienceDirect

Procedia Structural Integrity 64 (2024) 2013–2020

Structural Integrity Procedia

www.elsevier.com/locate/procedia

SMAR 2024 – 7th International Conference on Smart Monitoring, Assessment and Rehabilitation of Civil Structures

Strengthening of bridges with iron-based shape memory alloy bars embedded in UHPFRC

A. Lemos[a,b]*, C. Czaderski[a], I. Markovic[c], J. Michels[d], W. Kaufmann[b]

[a]*Empa, Swiss Federal Laboratories for Materials Science and Technology, Ueberlandstrasse 129, Dübendorf 8600, Switzerland*
[b]*ETH Zurich, Stefano-Franscini-Platz 5, Zurich 8093, Switzerland*
[c]*OST, University of Applied Sciences of Eastern Switzerland, Oberseestrasse 10, Rapperswil-Jona 8640, Switzerland*
[d]*re-fer AG, Riedmattli 9, Seewen 6423, Switzerland*

Abstract

Bridges are designed for a service life of up to 100 years. A significant number of structures still in use lack the required levels of structural safety, either due to deterioration or because older design codes are partly obsolete. With the increasing focus of the construction industry towards sustainability and circularity, there is a trend to develop innovative and efficient strengthening methods that enable the rehabilitation of under-designed or damaged structural components rather than rebuilding new structures. To this end, this paper presents a research project aiming at developing a new method for flexural strengthening of bridge decks, which consists in applying a layer of Ultra-High Performance Fibre Reinforced Concrete (UHPFRC) reinforced with Iron-based Shape Memory Alloy (Fe-SMA) ribbed bars on top of the existing Reinforced Concrete (RC) structure. The Fe-SMA bars are activated through heating, ultimately leading to the development of prestressing forces.
To analyse this novel technology, a case study is developed. The performance of the new system is compared to a strengthening using B500B steel reinforcing bars embedded in UHPFRC, highlighting the main advantages of the new method. Furthermore, the bond behaviour of Fe-SMA bars embedded in UHPFRC is characterised in detail through short pull-out tests. Design parameters such as the temperature of activation of Fe-SMA and concrete cover thickness are studied. The bond shear stress-slip relationships show very high bond strengths for all tested covers, even after a slight deterioration of the bond properties resulting from the heating.

Keywords: RC bridges; Flexural strengthening; UHPFRC; Fe-SMA; Bond-slip behaviour

* Corresponding author. Tel.: +41 78 208 0033
E-mail address: angela.lemos@empa.ch

10.1016/j.prostr.2024.09.284

1. Introduction

Concrete structures are typically designed to guarantee a life span of 50-100 years. Hence, a large number of existing structures may present significant deterioration and require rapid intervention. Furthermore, many intact structures do not comply with modern design codes, e.g. due to higher traffic loads and stricter requirements to prevent brittle failure. It is of public interest to develop sustainable, economical and easy-to-apply strengthening solutions as tax-payers' money is invested in maintenance, repair and strengthening of public structures and traffic disruptions cause high societal cost and greenhouse gas emissions (Hanson and Noland 2015).

Commonly used strengthening techniques for sagging moments include the use of externally bonded (EB) carbon-fibre reinforced polymers (CFRP) and Near-Surface Mounted (NSM) techniques in which small strips are bonded in previously chiselled grooves on the concrete surface (RILEM 2016). For strengthening components subjected to hogging moments, the established solution of adding conventional reinforcing bars in the top layer requires reprofiling the existing concrete and adds significant weight to ensure adequate cover. These issues can be mitigated by casting a top layer of Ultra-High Performance Fibre Reinforced Concrete (UHPFRC) reinforced with conventional reinforcing bars (Brühwiler and Bastien-Masse 2015, Zhang et al. 2020).

This paper presents an innovative method replacing the conventional steel reinforcement in the UHPFRC layer with Iron-based Shape Memory Alloy (Fe-SMA) ribbed bars, combining the advantages of UHPFRC with the benefits of the prestressing capabilities of Fe-SMA for flexural strengthening applications. UHPFRC is a fine-grained mixture characterised by greatly improved tensile and compressive behaviours when compared to Normal Concrete (NC) (Oesterlee 2010, Spasojević 2008). Its low permeability properties make this material even more interesting for bridge applications as no water-proofing barrier would need to be applied following the strengthening works. Iron-based shape memory alloys (Fe-SMA) have a special interest in Civil engineering applications due to their higher stiffness compared to Ni-Ti alloys and their lower cost (Cladera et al. 2014, Czaderski et al. 2014). After applying an initial deformation above the elastic limit – referred to as prestraining stage – these alloys partially recover their initial shape by heating the material above a specific temperature, defined as the Austenite's start temperature, A_s. The heating-cooling cycle is called activation. If restrained upon heating, these alloys develop internal stresses (referred to as recovery stress) which can be used for prestressing the parent structure.

The use of prestressed solutions enables carrying a part of the dead load of the strengthened structure, potentially allowing to partially recover cracks on deteriorated elements or to uplift components that exhibit excessive deformations. Recent studies have proven the feasibility of reinforcing concrete structures by applying a top layer of mortar prestressed with memory-steel (cover replacement method CR) as well as by the NSM method (Schranz et al. 2021). This way of applying prestress has a significant interest for on-site applications as there is no need for anchor heads, hydraulic jacks or additional mechanical devices during the prestressing stages.

2. Case study

2.1. Non-linear cross section analysis of a bridge deck

In order to analyse a realistic situation, a common twin T-girder cross-section bridge (overpass) was designed to have a transverse bending resistance deficit of about 15%. The total length of the overpass is assumed to be 75 m and its total width is 14 m. The applied traffic loads and design internal actions were calculated based on the SIA260 and SIA261 standards (SIA260:2013 , SIA261:2020). Partial safety factors were applied accordingly.

Several variants were developed for the strengthening of the parent structure by varying the thickness of the UHPFRC layer (40 mm, 50 mm, 60 mm), the reinforcement ratio of the additional steel layer (ϕ16 mm, spaced at 125 mm, 200 mm and 250 mm) and the type of steel (B500B or Fe-SMA).

Finally, the following configurations (also displayed in Fig. 1) were chosen for comparison:

- Solution 1) with ϕ16 mm B500B reinforcing bars spaced at 12.5 cm centres in a 60 mm UHPFRC layer
- Solution 2) with ϕ16 mm Fe-SMA reinforcing bars spaced at 25 cm centres in a 40 mm UHPFRC layer

The design of both strengthening solutions ensures a similar behaviour under serviceability limit states (e.g., similar stress amplitudes in the internal steel and similar strains at the outermost layer of UHPFRC).

Fe-SMA bars are only installed above the main girders while the central part is covered with conventional strengthening steel, given the fact that the application of prestress at the top would not be beneficial in the span.

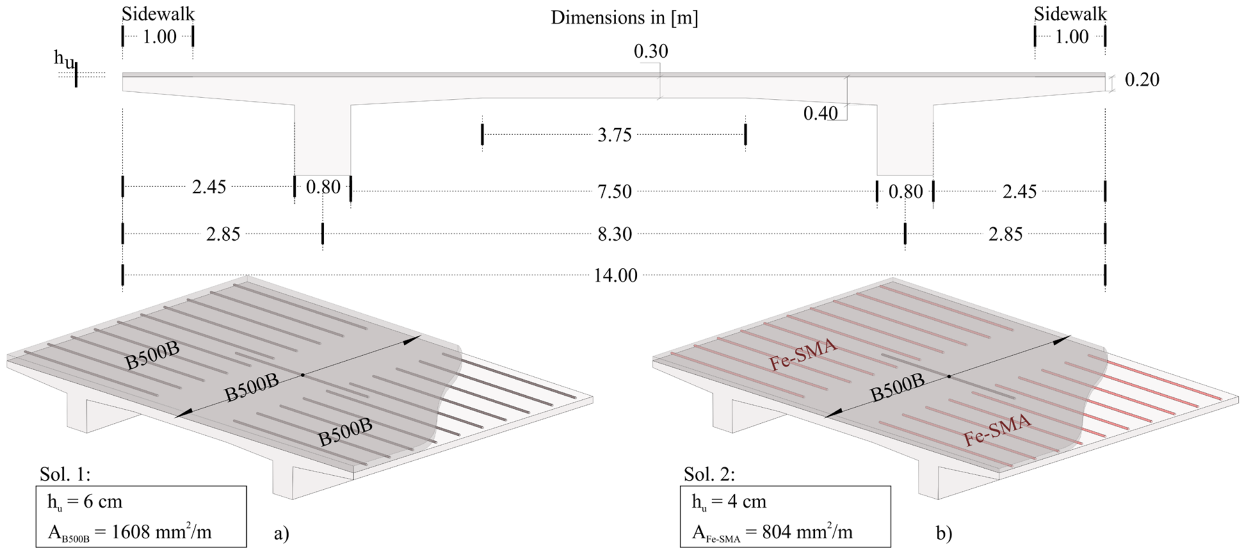

Fig. 1. Final configurations obtained for: a) Solution 1: UHPFRC + B500B; b) Solution 2: UHPFRC + Fe-SMA.

Both presented solutions showed very good results in terms of load bearing capacity and cracking moments and led to comparable fatigue loading of the internal steel. Fig. 2 shows the moment-curvature (M-φ) relationships obtained for the unstrengthened and strengthened cross sections and Table 1 compares the main design parameters. The characteristic points highlighted in the M-φ relationships were determined analytically based on cross section analysis, accounting for the non-linear behaviour of the different materials involved. The stress-strain curves adopted for conventional steel are based on existing standards (SIA262:2013) whereas the curves for Fe-SMA steel are based on experimental data obtained during loading, following the activation stage (Schranz et al. 2019). The material safety coefficients recommended in the Swiss standards were adopted.

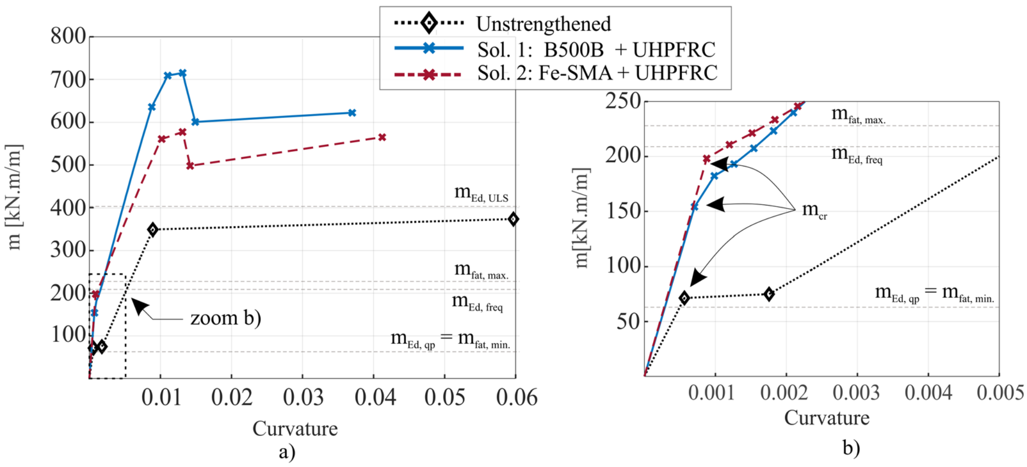

Fig. 2. Moment-curvature relationships for unstrengthened and strengthened solutions: a) overall behaviour until failure; b) detailed illustration (area marked in a) of the behaviour under service and fatigue load. Load combinations: ULS = ultimate limit state of structural safety; freq = frequent; qp = quasi-permanent; fat = fatigue.

Table 1. Comparison of main design parameters.

	Original Structure	Solution 1	Solution 2
Layer thickness, h_U (*mm*)	-	60	40
Additional reinforcement area – additional layer	-	Φ16, esp. =12.5cm	Φ16, esp. = 25cm
Resistance at ULS – m_{Rd} (*kN.m/m*)	373	715	577
Cracking moment – m_{cr} (*kN.m/m*)	78	151	190
Decompression moment – $m_{decomp.}$ (*kN.m/m*)	0	0	80
$\varepsilon_{max,\ UHPFRC}$ (*‰*) at SLS	-	0.7 ‰	0.65 ‰
Stress amplitude in internal steel – $\Delta_{\sigma 1,fat}$ (*MPa*)	213	57	46
Max. fatigue stress in internal steel – $\sigma_{1,max,fat}$ (*MPa*)	216	62	50
Max. stress levels in additional layer – $\sigma_{3,max,fat}$ (*MPa*)	-	47	335

2.2. Discussion of the results

By analysing Fig. 2 and Table 1, it is possible to conclude that both solutions largely provide the load bearing capacity required to ensure structural safety (ULS). Nonetheless, Solution 2 provides a better performance at serviceability limit states (SLS) despite using only half the amount of steel and a significantly thinner UHPFRC layer.

The cracking moment, m_{cr}, increased significantly for both strengthened solutions but it is still 26% higher for the prestressed Solution 2. More importantly, Solution 2 ensures an uncracked behaviour up to the decompression moment, $m_{decomp} = 80\ KN.m/m$, for the entire service life of the retrofitted structure. The decompression moment refers to the state at which the outermost fibre on the concrete section experiences zero strains. Further increasing the applied moments after this point, initiates tensile strains in the concrete section.

The strain level at the outermost fibre of the UHPFRC layer, ε_{UHPFRC}, is important to guarantee the sealing properties of this material. According to (SIA2052:2016), it should be kept below 1‰ thus avoiding the installation of an additional waterproofing barrier. The strain levels obtained for both solutions are similar (slightly lower for Solution 2) and both thus comply with this limit at the service load level.

The stress amplitudes $\Delta_{\sigma s1}$ in the internal steel correspond to the difference between the stresses under the maximum and minimum fatigue loads, calculated based on (SIA261:2020). In accordance to (SIA262:2013) the limit value for a ϕ20 mm reinforcing bar is $\Delta\sigma_{sd,D}$ = 116 MPa. Both strengthened solutions easily comply with the standard requirements.

As the Fe-SMA bars are prestressed in Solution 2, the maximum stresses under fatigue load in the additional layer of reinforcement are considerably higher, 335 MPa, when compared to the stresses applied to the additional layer when normal steel is deployed, 47 MPa. It is therefore important that the fatigue performance of Fe-SMA bars complies with high standard requirements. Ghafoori et al. 2017 proposes a model for fatigue design. Based on the referred model, for a mean stress value of 335 MPa and an alternate stress of roughly 50 MPa, safety if guaranteed.

2.3. Activation methods

There are currently two possible heating methods used for the activation of Fe-SMA bars: i) electrical resistive heating, where the bars are fully embedded in the UHPFRC layer; or ii) heating in between anchorages (e.g. with a gas torch device). In Fig. 3 the two options are depicted, where approach (a) requires resistive heating while (b) enables both methods.

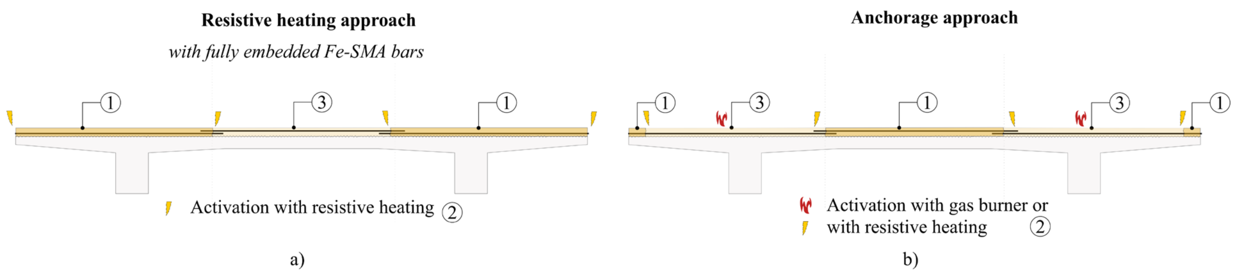

Fig. 3. Activation methods for activating the Fe-SMA bars: a) resistive heating approach; b) anchorage approach.

When using the "resistive heating approach" depicted in Fig. 3a), the surfaces on the left and right sides of the bridge are cast first (1). Once the cementitious material has hardened, a power source is used to heat the reinforcing bars thus triggering the shape memory effect (2). Subsequently, the UHPFRC is cast along the remaining surface of the bridge (3). This approach has the advantage of requiring less construction joints.

Conversely, when using the "anchorage approach" (Fig. 3b), the end anchorages and mid-surface are cast first (1) and, after hardening, the bars are heated with a direct heating source or with resistive heating (2). The recovery stress that builds up in the Fe-SMA bars is transmitted to the anchorages which must resist the induced stresses. Finally, the surface in-between the anchorages is cast (3).

After recent findings by the author (not yet published), it was possible to conclude that it is not feasible to activate the Fe-SMA bars after they are fully embedded in the UHPFRC given that a great amount of energy is transferred to the UHPFRC matrix, ultimately resulting in long heating times and premature cracks that spread longitudinally along the UHPFRC surface. The latter is explained by the high thermal conductivity coefficient of UHPFRC which can, in certain cases, reach 6 $W \cdot m^{-1}K^{-1}$, depending on the UHPFRC composition (compared to 1.0-2.0 $W \cdot m^{-1}K^{-1}$ for NC). Presumably, the temperature gradient from the inner section in contact with the Fe-SMA bars towards the outside causes hoop stresses and ultimately longitudinal cracks that undermine the efficiency of the method and the sealing properties of UHPFRC. For this reason, the "anchorage approach" is recommended by the authors.

3. Pull-out test campaign

3.1. Test set-up and experimental procedure

A series of pull-out tests on reinforcing bars embedded in UHPFRC cubes, with short bonded lengths (similar to (RILEM-TC 1994), was carried out. Design parameters such as the cover thickness and the influence of heating on the deterioration of the bond resistance were evaluated. Table 2 and Fig. 4 summarise the experimental programme. In order to accurately capture the bond behaviour without premature failure of the reinforcing bar, the bonded length was limited to about 1.5d (being d the diameter of the reinforcing bar). Hence, a bonded length of 25 mm was chosen for all the specimens and the size of the adapted Rilem cubes was reduced to 15 cm. Bars with a diameter of about ϕ16 mm were used for all tests. Along the unbonded length, the bars were encased in a plastic sleeve.

Table 2: Summary of the short embedment length pull-out tests. Fe-SMA^H indicates that the Fe-SMA bar underwent heating.

Group	Specimen	Configuration	Cover [mm]	Bar material
PO-4	7-8	B	44	Fe-SMA
PO-5	9-10	C	24	Fe-SMA
PO-6	11-12	B	44	Fe-SMA^H
PO-7	13-14	C	24	Fe-SMA^H

The tests were performed in a servo-hydraulic testing machine of type Amsler. The specimens were placed on the machine's traverse and the reinforcing bar was clamped at the bottom. The load was applied at displacement control by moving the machine's crossbeam upwards, with a constant displacement rate of 0.008 mm/s. In order to guarantee a uniform distribution of stresses between the cube and the steel plate, a 3 mm rubber layer was placed on top of the steel plate. The sampling frequency was 5Hz. Digital Image Correlation (DIC) was used to capture eventual cracks on the UHPFRC surface.

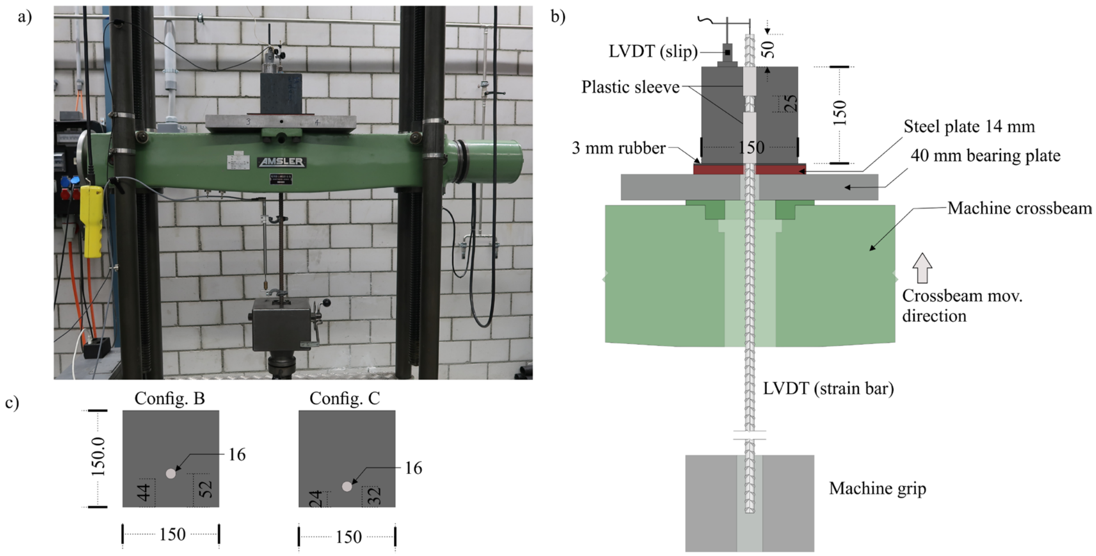

Fig. 4: Test setup: a) picture taken before testing; b) instrumentation used in the experiments; c) Configurations B and C. Dimensions in mm.

3.2. Material characterization

Table 3 summarises the UHPFRC mix composition and the main material properties.

Table 3: UHPFRC mixture composition and material properties

UHPFRC mixture composition			
Density	2606	[kg/m3]	
Premix (inc. CEM type I)	2100	[kg/m3]	
Admixtures	31	[kg/m3]	
Steel fibres (L_f =12.5mm; d_f = 0.175mm)	300	[kg/m3]	(3.8 % in volume)
Water	175	[kg/m3]	
UHPFRC - compressive strength and young modulus			
Curing regime	20°C; in water		20°C; in water
Age [days]	28		36
Cube compressive strength [Mpa]	168 (+/- 1.8)		176.5 (+/- 2.6)
Young Modulus [GPa]	52.7 (+/- 0.7)		-
Density [kg/m^3]	2571 (+/- 6)		2540 (+/- 12.8)
Steel reinforcement			
Steel type		Fe-SMA	
Nominal diameter [mm]		16.8	
Relative rib area, f_R		0.055	
Young Modulus [GPa]		165 (+/- 15)	

3.3. Pull-out tests results

Nominal bond shear stress-slip relationships were derived assuming a uniform bond stress along the short embedment length:

$$\tau_b = \frac{F}{\pi \cdot d_s \cdot l_b} \quad (1)$$

, where τ_b denotes the uniform bond shear stress, F the applied load, d_s the reinforcing bar nominal diameter and l_b the embedment length. In Fig. 5, the main results are presented.

The peak bond strength obtained for all specimens was the range of 42…57 MPa (see Fig. 5a), hence significantly higher than the design values recommended by the MC2010 for normal concrete (NC) (FIB-CEB 2010). The MC bond relationships are thus inadequate for fitting the experimental results of pull-out tests using UHPFRC, as opposed to NC. A similar result was reported in (Marchand et al. 2015).

The specimens belonging to Group PO6 (Specimens 11 and 12) were heated up to 200 °C and, after cooling, the pull-out tests were performed. Comparing the results obtained for Groups PO4 and PO6 (44 mm cover) - Fig. 5b), roughly a 20% reduction of the peak bond stress was caused by the heating of the Fe-SMA bars. DIC captured the appearance of splitting cracks on the surface of the UHPFRC cubes of Group PO6, and a crack recovery of more than 60% was registered with the reduction of the applied load after failure. No cracks were identified for the specimens in group PO4 (Specimens 7 and 8) which justifies the higher load obtained.Contrary to what was observed in the groups PO4 and PO6, no significant peak bond stress reduction was obtained for the specimens with a cover of 24 mm (groups PO5 and PO7) - Fig. 5c), even though the specimens in Group PO7 also underwent heating. In this case, all 4 specimens exhibited surface cracks, which can be explained by the reduced cover.

When analysing the influence of the cover thicknesses in unheated specimens – Groups PO4 (44 mm cover) and PO5 (24 mm cover) – a reduction of the peak bond strength is observed for the 24 mm cover. Conversely, the residual bond resistance seems to be higher for Group PO5, and reducing at a slower deterioration rate.

Regarding the heated specimens – Groups PO6 (44 mm cover) and PO7 (24 mm cover) – no significant differences in the peak stresses were observed, which can be justified by the mixed failure mode that was obtained in both configurations (pull–out and splitting of the UHPFRC cover).

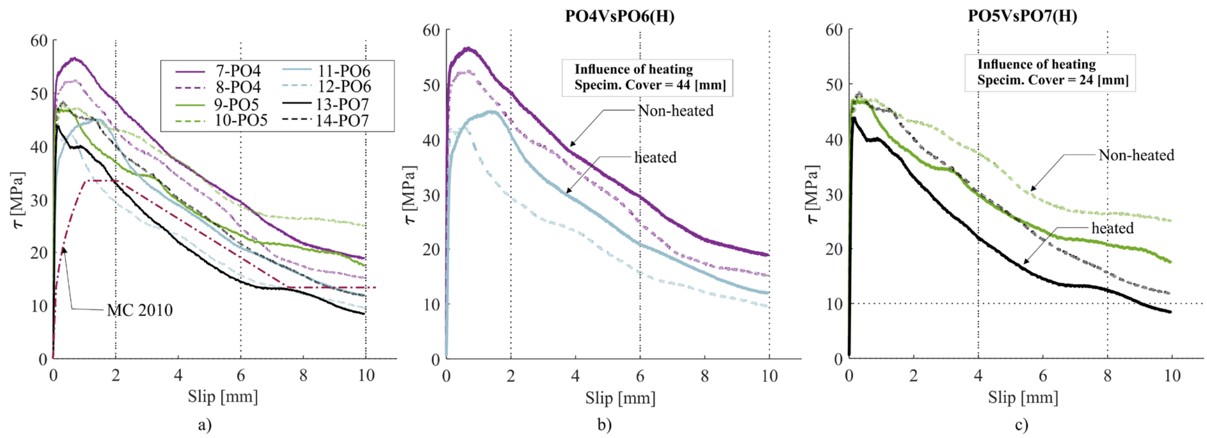

Fig. 5: Bond - slip relationships: a) Pull-out tests 7 to 14; b) specimens with a steel cover of 44mm; c) specimens with a steel cover of 24mm;

4. Conclusions and outlook

In the present paper, a new strengthening method is presented, highlighting its advantages compared to more conventional methods. The capabilities of Fe-SMA to recover its shape upon heating enables the development of prestressed strengthening methods targeting existing structures with serviceability deficits. Besides having a great potential to reduce crack widths and to partly recover deflections of structural components, the amount of materials can be reduced. In the given case study, the steel quantity was reduced to half and the UHPFRC layer thickness was reduced from 60 mm to 40 mm. Nonetheless, the cracking moment using the innovative method was still roughly 26% higher and, more importantly, the prestressed solution ensures an uncracked behaviour under quasi-permanent loads.

In order to characterise the bond behaviour of ribbed Fe-SMA bars inside UHPFRC, a series of short pull-out tests was carried out. A peak bond stress reduction up to 20% was obtained after heating the Fe-SMA bars inside UHPFRC. Notwithstanding, the obtained values (42…57 MPa) are still significantly higher than the values recommended by design codes for normal concrete. A combined pull-out and splitting failure was observed for the specimens of Groups PO5, PO6 and PO7, whereas for Group PO4, pull-out failure governed. As only two tests were performed for each set of parameters, i.e., each pullout test group was composed of two specimens, the results should be addressed carefully. This also applies to the assumed constant bond stresses along the bonded length and the test configuration not being fully representative of the confinement conditions in real structures. Nonetheless, the experiments provide a good insight on how the different parameters impact the bond shear stress-slip relationships and, by following a simplified test procedure recommended by existing codes, comparisons with similar tests in the literature are possible. In future test campaigns, the referred test limitations will be addressed, longer bond lengths will be tested and Distributed Fibre Optical Sensing technologies will be used in order to record the bond stresses continuously along the embedment lengths. Finally, pertinent bond shear stress-slip laws will be proposed on this basis.

Acknowledgements

The authors thank the financial support of the Swiss Innovation Agency, Innosuisse – Project Number: 56234.1 IP-ENG – and the industrial partners cemsuisse and re-fer AG for providing the material used in this research.

References

Brühwiler, E. and Bastien-Masse, M. (2015) Strengthening the Chillon viaducts deck slabs with reinforced UHPFRC. In Paper Presented to the IABSE Conference – Structural Engineering: Providing Solutions to Global Challenges, Switzerland.

Cladera, A., Weber, B., Leinenbach, C., Czaderski, C., Shahverdi, M. and Motavalli, M. (2014) Iron-based shape memory alloys for civil engineering structures: An overview. *Construction and Building Materials, 63*, pp. 281-293.

Czaderski, C., Shahverdi, M., Brönnimann, R., Leinenbach, C. and Motavalli, M. (2014) Feasibility of iron-based shape memory alloy strips for prestressed strengthening of concrete structures. *Construction and Building Materials, 56*, pp. 94-105.

FIB-CEB (2010) *fib Model Code for Concrete Structures 2010*.

Ghafoori, E., Hosseini, E., Leinenbach, C., Michels, J. and Motavalli, M. (2017) Fatigue behavior of a Fe-Mn-Si shape memory alloy used for prestressed strengthening. *Materials & Design, 133*, pp. 349-362.

Hanson, C. S. and Noland, R. B. (2015) Greenhouse gas emissions from road construction: An assessment of alternative staging approaches. *Transportation Research Part D: Transport and Environment, 40*, pp. 97-103.

Marchand, P., Baby, F., Khadour, A., Battesti, T., Rivillon, P., Quiertant, M., Nguyen, H.-H., Généreux, G., Deveaud, J.-P., Simon, A. and Toutlemonde, F. (2015) Bond behaviour of reinforcing bars in UHPFRC. *Materials and Structures, 49*(5), pp. 1979-1995.

Oesterlee, C. (2010) *Structural Response of Reinforced UHPFRC and RC Composite Members*. Unpublished Doctoral Thesis, EPFL, Lausanne.

RILEM-TC (1994) Bond test for reinforcement steel. 2. Pull-out test. In Paper Presented to the RILEM Recommendations for the Testing and Use of Constructions Materials.

RILEM (2016) *Design Procedures for the Use of Composites in Strengthening of Reinforced Concrete Structures, RILEM State-of-the-Art Reports,* Springer Dordrecht.

Schranz, B., Czaderski, C., Shahverdi, M., Michels, J., Vogel, T. and Motavalli, M. (2019) Ribbed iron-based shape memory alloy bars for pre-stressed strengthening applications. In Paper Presented to the IABSE Symposium 2019 Guimarães: Towards a Resilient Built Environment - Risk and Asset Management, Guimarães, Portugal.

Schranz, B., Michels, J., Czaderski, C., Motavalli, M., Vogel, T. and Shahverdi, M. (2021) Strengthening and prestressing of bridge decks with ribbed iron-based shape memory alloy bars. *Engineering Structures, 241*.

SIA260:2013 Bases pour l'élaboration des projets de structures porteuses (SIA 260:2013). in,Zürich.

SIA261:2020 Actions sur les structures porteuses (SIA 261:2020). in,Zürich.

SIA262:2013 Concrete Structures (SIA 262:2013). in,Zurich.

SIA2052:2016 Béton fibré ultra-performant (BFUP) - Matériaux, dimensionnement et exécution (SIA 2052:2016). in,Zürich.

Spasojević, A. (2008) *Structural implications of ultra-high performance fibre-reinforced concrete in bridge design*. Unpublished Doctoral Thesis EPFL, no 4051 (2008), Lausanne.

Zhang, Y., Li, X. L., Zhu, Y. P. and Shao, X. D. (2020) Experimental study on flexural behavior of damaged reinforced concrete (RC) beam strengthened by toughness-improved ultra-high performance concrete (UHPC) layer. *Composites Part B-Engineering, 186*.